Physica B ▮ (▮▮▮▮) ▮▮▮–▮▮▮

Contents lists available at SciVerse ScienceDirect

Physica B

journal homepage: www.elsevier.com/locate/physb

Electrical transport properties of manganite powders under pressure

M.G. Rodríguez [a], A.G. Leyva [b], C. Acha [a,*]

[a] Laboratorio de Bajas Temperaturas, Departamento de Física, FCEyN, UBA, and IFIBA (CONICET), Ciudad Universitaria, (C1428EHA) Buenos Aires, Argentina
[b] Gerencia de Investigación y Aplicaciones, CAC, Comisión Nacional de Energía Atómica, Gral Paz 1499, 1650 San Martín, Buenos Aires, Argentina

ARTICLE INFO

Keywords:
Manganites
Nanoparticles
Pressure effects
Electronic transport

ABSTRACT

We have measured the electrical resistance of micrometric to nanometric powders of the $La_{5/8-y}Pr_yCa_{3/8}MnO_3$ (LPCMO with $y=0.3$) manganite for hydrostatic pressures up to 4 kbar. By applying different final thermal treatments to samples synthesized by a microwave assisted denitration process, we obtained two particular grain characteristic dimensions (40 nm and 1000 nm) which allowed us to analyze the grain size sensitivity of the electrical conduction properties of both the metal electrode interface with manganite (Pt/LPCMO) and the intrinsic intergranular interfaces formed by the LPCMO powder, conglomerate under the only effect of external pressure. We also analyzed the effects of pressure on the phase diagram of these powders. Our results indicate that different magnetic phases coexist at low temperatures and that the electrical transport properties are related to the intrinsic interfaces, as we observe evidences of a granular behavior and an electronic transport dominated by the Space Charge limited Current mechanism.

© 2011 Elsevier B.V. All rights reserved.

1. Introduction

Up to now there have been many studies trying to shown which is the particular influence of grain size on the properties of ceramic manganites [1,2]. It is clear that, by reducing the grain size of the sample, the surface to volume ratio increases, having clear implications in their physical properties. Considering nearest neighbors, magnetic interactions are different in bulk than in the surface layer. Also impurities and oxygen content as well as the crystal structure can also be different, modifying particularly transport properties for their large sensitivity to the intergrain coupling. Finally, the phase transitions may be modified, affecting particularly most of the physical properties of these phase separation systems. Regarding transport properties, it is well known fact that manganites in the paramagnetic state (PM) have a semiconducting-like temperature dependent resistance. On the other hand, if we are dealing with samples in powder form, only held together by the application of external pressure (P), we would expect that this granularity will dominate the behavior of the electrical conduction, by determining an extrinsic mean free path of carriers or the tunneling mechanism between grains. In this paper we present resistance measurements as a function of temperature of $La_{5/8-y}Pr_yCa_{3/8}MnO_3$ (LPCMO with $y=0.3$) powders with two distinct grain sizes (1 μm and 40 nm) Thus, by comparison, we want to explore the influence of nanostructuration on the electrical transport properties, to determine the main mechanism that regulates the conductivity between grains and to determine the sensitivity to external pressure of the magnetic ordering of this compound.

2. Experimental

In this paper we study the ceramic manganite $La_{5/8-y}Pr_yCa_{3/8}MnO_3$ (LPCMO with $y=0.3$), whose morphology corresponds to a non-sintered powder. These samples were synthesized following a microwave assisted denitration process [3] and a final heat treatment at different temperatures to obtain grain sizes nearly two orders of magnitude different: Sample A, with a final sintering treatment of 4 h at 1400 °C, with a grain size diameter (D_g) of 1−2 μm and Sample B, treated at 800 °C for 10 min with D_g close to 40 nm. From room temperature down to 50 K this compound presents several magnetic transitions and a complicated phase separation scenario. A magnetic characterization and the effects of hydrostatic pressure on the different magnetic orderings can be found in a previous work [4].

In order to study the electrical transport properties of the powders at different pressures two different techniques were used: for small pressures ($P \leq 0.4$ kbar) the powders were introduced inside a 2 mm diameter pyrophyllite ring with Pt wires, the whole arranged in a Bridgman-like configuration, where a small uniaxial pressure was applied just to ensure the electrical conductivity of the powder. For higher pressures, the inner volume of a plastic (Teflon) cylinder was filled with the sample's powder

* Corresponding author.
E-mail address: acha@df.uba.ar (C. Acha).

0921-4526/$ - see front matter © 2011 Elsevier B.V. All rights reserved.
doi:10.1016/j.physb.2011.12.046

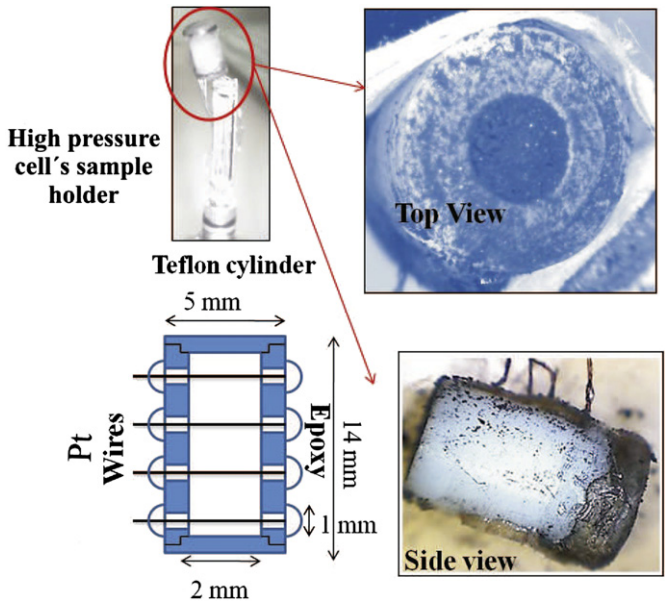

Fig. 1. Setup to measure the resistance of powder samples under hydrostatic pressure. Left panel: Part of the inner sample holder of the hydrostatic cell with the Teflon cylinder on top and its sketch. Right panel: Different views of the Teflon cylinder filled with the LPCMO powders.

(shown in Fig. 1) and pressurized inside a piston-cylinder hydrostatic cell. The plastic cylinder has two removable lids and four equidistant holes through its walls, ranging from side to side along its diameter, where Pt leads were introduced to perform the resistance measurements using a standard four terminal DC technique. To avoid overheating and non-linear effects the exciting current was regulated to keep the voltage drop across the sample below 10 mV. *IV* characteristics were also measured using the same configuration. The cylinder and all its holes were carefully sealed by using a low temperature resistent epoxy in order to avoid that the pressurizing fluid (50% and 50% kerosene and transformer oil) mixes with the sample preventing its electrical continuity. The proper increase of pressure inside the cylinder with increasing the pressure of the fluid was successfully checked by measuring the electrical resistance of a manganin wire placed inside the cylinder with steatite powder as the inner transmitting medium. Only a small pressure range can be studied; up to 0.4 kbar for the Bridgman-like setup, due to the maximum allowed uniaxial stresses. For the hydrostatic cell, a minimum pressure (in some cases up to $\simeq$ 2 kbar) was required to have low contact resistances in order to allow the resistance measurements, and, due to the pressure cell inner dimensions, the maximum attained pressure was 4 kbar.

3. Results and discussion

The temperature dependence of resistance of both samples (A and B) at different pressures can be observed in Fig. 2. Resistance measurements shown here were taken on warming. Measurements on cooling showed a different path due to hysteresis effects associated with the first-order-type transition in a system with two-phase coexistence [5]. Both samples show a high resistance value when compared to sintered ceramic samples of similar geometric factors [5]. Sample A shows a semiconducting-like dependence in the paramagnetic state and very well defined transitions to the ferromagnetic ordering and to the charge ordered antiferromagnetic state, corresponding to the temperatures labeled T_{c2},T_{c1} and T_N, respectively. A metallic-like

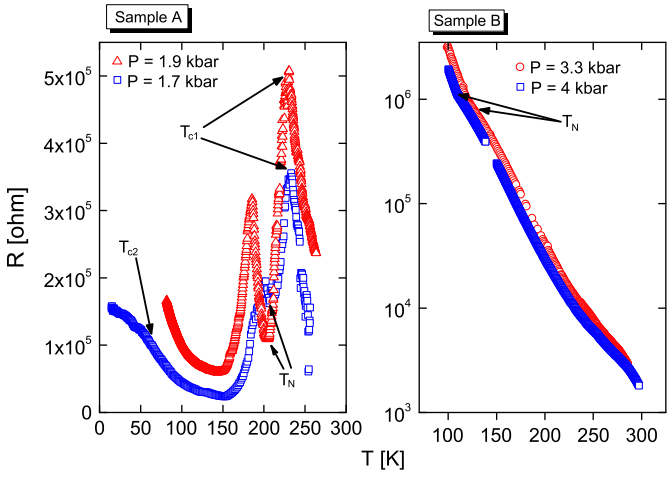

Fig. 2. Temperature dependence of the resistance of Sample A and B at different pressures. The transition temperatures are indicated for each case (T_{c1}, T_N and T_{c2} for Sample A, and only T_N for Sample B).

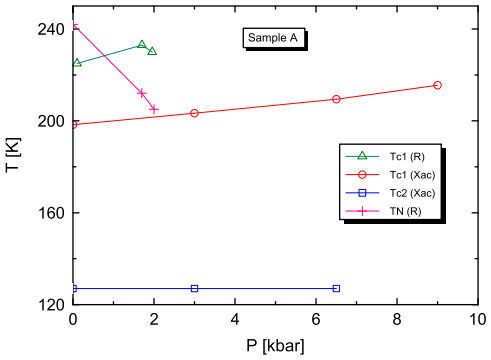

Fig. 3. Phase diagram of Sample A. The transition temperatures obtained previously by AC susceptibility [4] are also included for comparison.

conduction can be observed in two intermediate temperature regions, arbitrarily given rise to a peak in the resistance, not necessarily associated with a magnetic order transition but rather to the temperature dependence of a competing distribution of metallic and insulator regions developed as a consequence of the phase separation scenario.

As a clear difference with the resistance dependence for sintered samples, the ground state of Sample A seems to be insulator, instead of metallic [6]. On the other hand, Sample B shows a quite different resistance dependence, which is essentially semiconducting-like for the whole temperature range. Nevertheless, by analyzing the logarithmic derivative of the resistance (no shown here), the ferromagnetic onset of T_{c1} seems to be located over 300 K. At T_N the resistance substantially increases, reaching values over our experimental capacity, preventing the measurement down to low temperatures.

In Figs. 3 and 4 the obtained phase diagram can be seen. We also included for comparison the curves obtained in a previous paper [4] where we studied the pressure sensitivity of the magnetic ordering transitions by AC susceptibility. The transition temperatures measured by different techniques not necessarily coincides, but the general trend is maintained. In this sense, the CO-AF transition is quickly reduced by increasing the pressure while the FM transition increases softly. Here, by measuring the pressure sensitivity of the resistance, we confirm these previous results. Interestingly, from the magnetic studies, the FM transition developed at T_{c2} completely mask our capacity to detect the

Please cite this article as: M.G. Rodríguez, et al., Physica B (2011), doi:10.1016/j.physb.2011.12.046

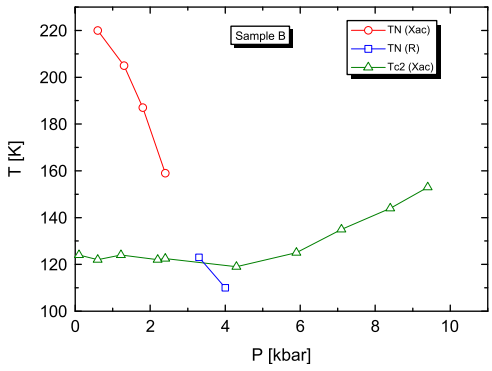

Fig. 4. Phase diagram of Sample B. The transition temperatures obtained previously by AC susceptibility [4] are also included for comparison. There were not evidences in the resistivity of the transitions at T_{c1} and T_{c2}.

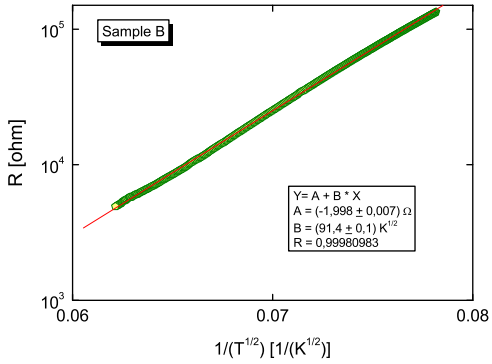

Fig. 5. Resistance of Sample B at 4 kbar as a function of $1/T^{0.5}$ in the paramagnetic temperature range. The line is a fit using Eq. (1).

existence of the AF transition in the case that $T_N \leq T_{c2}$. In contrast, the resistance measurements reveal that the CO-AF phase is still present up to 4 kbar, even for temperatures in that range, at least for Sample B. The pressure range of our measurements should be extended to generalize these results for both samples.

From the temperature sensitivity of the resistance, it was not possible to elucidate the dominant electrical transport mechanism for Sample A, as both the fits based on a semiconductor-like conduction and on the granular type gave reasonable results. However, for Sample B, we obtained a better match considering the granular conduction model [7,8] instead of the semiconducting one, as can be observed in Fig. 5. The expression we use to fit our data corresponds to:

$$\ln(R) = \frac{C_0}{T^{1/2}} = 4\left\{\frac{(\chi S^2 e^2)\left(1+\frac{1}{2\chi S}\right)}{\epsilon D\left(\frac{1}{2}D+S\right)k_b T}\right\}^{1/2}, \quad (1)$$

where $\chi^2 = 2m\Delta\phi/\hbar^2$, m and e are the electron's mass and charge, respectively, $\Delta\phi$ the energy difference between the effective barrier height and the electrons energy, k_b the Boltzmann constant, ϵ the dielectric constant of the insulator, D its characteristic grain size and S the grain separation distance, associated with the insulator layer between the conducting grains. A crude estimation of S can be performed, assuming that $\Delta\phi$ is in the 60–200 meV range (from the conductivity activation energy [9,10]) and $\epsilon \simeq$ 10–100. [11] The obtained value is in the 1–10 nm range, in a very good agreement with previous estimations [12].

We also analyze the *IV* characteristics in order to gain insight on the conduction mechanism between interfaces. We present in

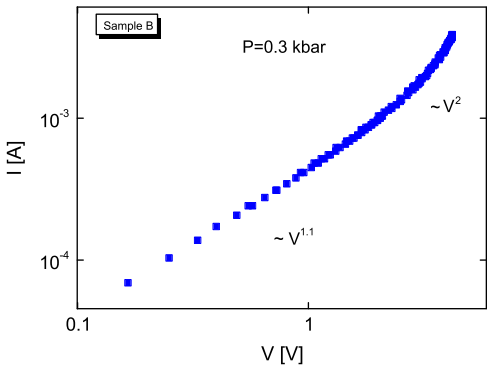

Fig. 6. *IV* characteristics at room temperature for Sample B at 0.3 kbar. A crossover from a nearly ohmic dependence to a $I-V^2$ law can be observed, typical of a SCLC conduction mechanism at granular interfaces.

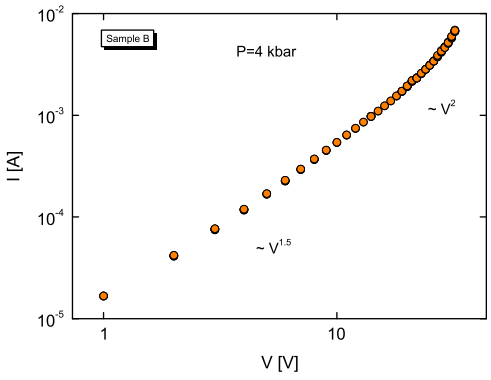

Fig. 7. *IV* characteristics at room temperature for Sample B at 4 kbar. As in Fig. 6 the obtained dependence is representative of a SCLC mechanism, where electrons are injected by good conducting zones into semiconductors in close electrical contact. Here, the crossover to a $I-V^2$ occurs at higher voltages indicating that pressure favors the conduction of the semiconducting zones.

Figs. 6 and 7 results for Sample B, although a similar behavior was obtained for Sample A. In both figures a non-linear dependence can be observed that evolves from a nearly ohmic relation to a power law with $I-V^2$.

This behavior is typical of the space charge limited currents (SCLC) mechanism, obtained for interfaces formed by good metals in contact with semiconductors [13]. It is interesting to note that the crossover to the quadratic dependence is shifted to higher voltage values with increasing pressure, indicating that pressure extend the ohmic behavior of the interface, probably by increasing the conductivity of the semiconductor [14]. As the *IV* characteristics were measured in a four terminal configuration, it is clear that the SCLC conduction is not only related to the interface formed by the Pt electrodes with the powder but it is essentially associated with the intrinsic interfaces formed between grains. As in the granular model that describes the temperature dependent resistance, the SCLC bulk conduction is revealing the existence of good metallic zones (grains) very well connected to a semiconducting layer (surface of grains).

4. Conclusions

We have measured, as a function of temperature and pressure, the electrical transport properties of LPCMO powders samples with grain sizes in the micrometric to nanometric scale. Both samples show a conduction behavior dominated by the interfaces, with non-linearities based on the SCLC mechanism and a conduction regime

Please cite this article as: M.G. Rodríguez, et al., Physica B (2011), doi:10.1016/j.physb.2011.12.046

ARTICLE IN PRESS

determined by their extrinsic granularity. Within the granular model, we made a crude estimation of the insulator layer obtaining a value in the 1–10 nm range. Considering the magnetic order transitions, we obtain a phase diagram that confirms previous results obtained by magnetic measurements. Moreover, new results were obtained as we observed the coexistence of the CO-AF phase with the low temperature FM phase confirming the complex phase diagram of these phase separated compounds.

References

[1] R.D. Sánchez, J. Rivas, C. Vázquez-Vázquez, A. López-Quintela, M.T. Causa, M. Tovar, S. Oseroff, Appl. Phys. Lett. 68 (1996) 134.
[2] A. Dutta, N. Gayathri, R. Ranganathan, Phys. Rev. B 68 (2003) 054432.
[3] A. Leyva, P. Stoliar, M. Rosenbusch, V. Lorenzo, P. Levy, C. Albonetti, M. Cavallini, F. Biscarini, H. Troiani, J. Curiale, et al., J. Solid State Chem. 177 (2004) 3949.
[4] C. Acha, G. Garbarino, A.G. Leyva, Physica B 398 (2007) 212.
[5] M. Uehara, S. Mori, C.H. Chen, S.-W. Cheong, Nature (London) 399 (1999) 560.
[6] J.A. Collado, C. Frontera, J.L.G.-M. noz, C. Ritter, M. Brunelli, M.A.G. Aranda, Chem. Mater. 15 (2003) 167.
[7] P. Sheng, B. Abeles, Phys. Rev. Lett. 28 (1972) 34.
[8] P. Sheng, B. Abeles, Y. Arie, Phys. Rev. Lett. 31 (1973) 44.
[9] E. Dagotto, T. Hotta, A. Moreo, Phys. Rep. 344 (2001) 1.
[10] G. Garbarino, C. Acha, D. Vega, G. Leyva, G. Polla, C. Martin, A. Maignan, B. Raveau, Phys. Rev. B 70 (2004) 014414.
[11] J.L. Cohn, M. Peterca, J.J. Neumeier, Phys. Rev. B 70 (2004) 214433.
[12] J. Curiale, M. Granada, H.E. Troiani, R.D. Sánchez, A.G. Leyva, P. Levy, K. Samwer, Appl. Phys. Lett. 95 (2009) 043106.
[13] G. Dietz, W. Antpohler, M. Klee, R. Waser, J. Appl. Phys. 78 (1995) 6113.
[14] P.C. Joshi, S.B. Krupanidhi, J. Appl. Phys. 73 (1993) 7627.

Please cite this article as: M.G. Rodríguez, et al., Physica B (2011), doi:10.1016/j.physb.2011.12.046